Optical Kerr Effect in gold nanorods

Note: This is a preliminary version

dr Kamil Polok

1 UV/VIS

According to the Mie theory, the UV/VIS spectra contain both scattering and absorption contributions (see Fig 1, left). The absorption scales as R^3, whereas the scattering as R^6. For example for 20 nm nanoparticles the absorption cross section is two orders of magnitude larger than the scattering cross section, whereas for 100 nm nanoparticles the scattering cross section is twice as large as the absorption cross section [1]. The low wavelength part of the spectrum contains a contribution due to interband transitions (see Fig 1, right). Gold nanospheres in the size range commonly employed ($\sim$ 40 nm) exhibit an absorption cross-section 5 orders orders of magnitude higher than conventional absorbing dyes [2].

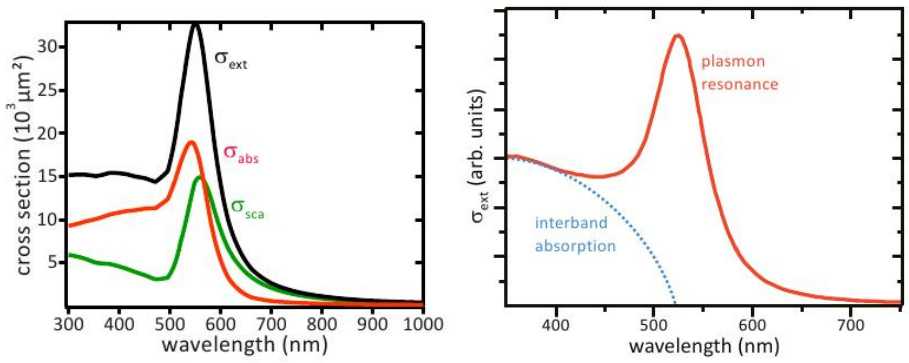

Figure 1: (Left) – Mie theory results. Calculated extinction (black), scattering (green) and absorption (red) cross sections for an 80 nm gold nanoparticle in water [1]; (Right) – Extinction spectrum of a colloidal suspension of 40 nm gold nanoparticles. The plasmon resonance is centered at 528 nm. The contribution of interband excitations is clearly seen for wavelengths below 520 nm [1].

In the case of nanorods, two peaks are observed in the spectrum, corresponding to the longitudinal (longer wavelength) and transverse (shorter wavelength) plasmon resonance (see Fig 2).

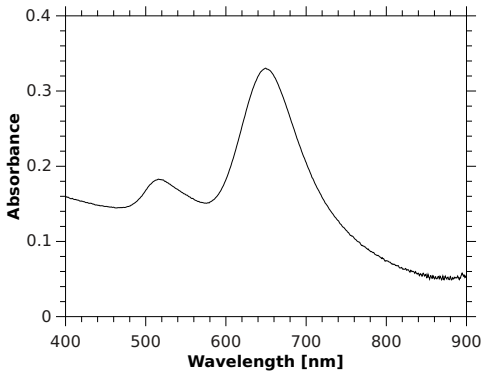

Figure 2: UV/VIS spectrum of 15x35 nm nanorods.

2 Nanoparticles OKE signal

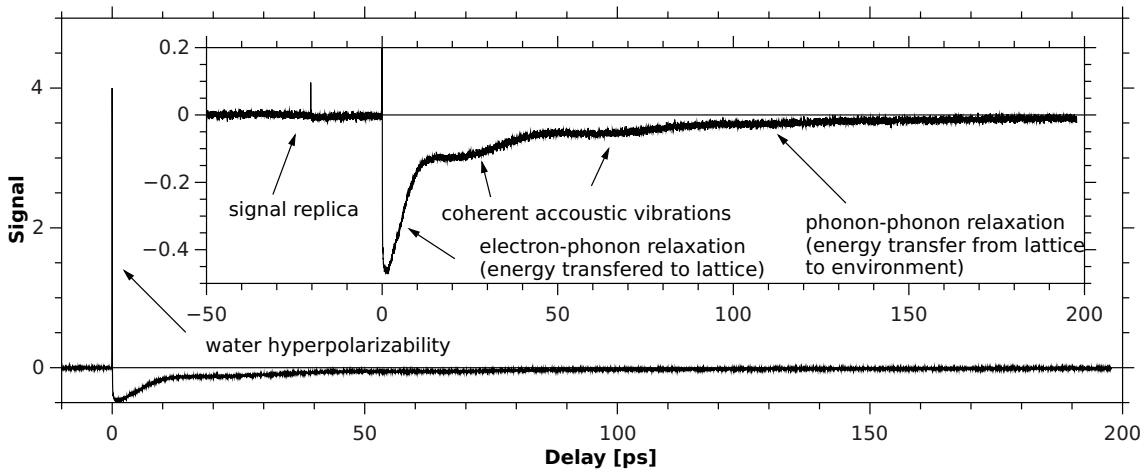

Figure 3: Example OKE signal of nanorods.

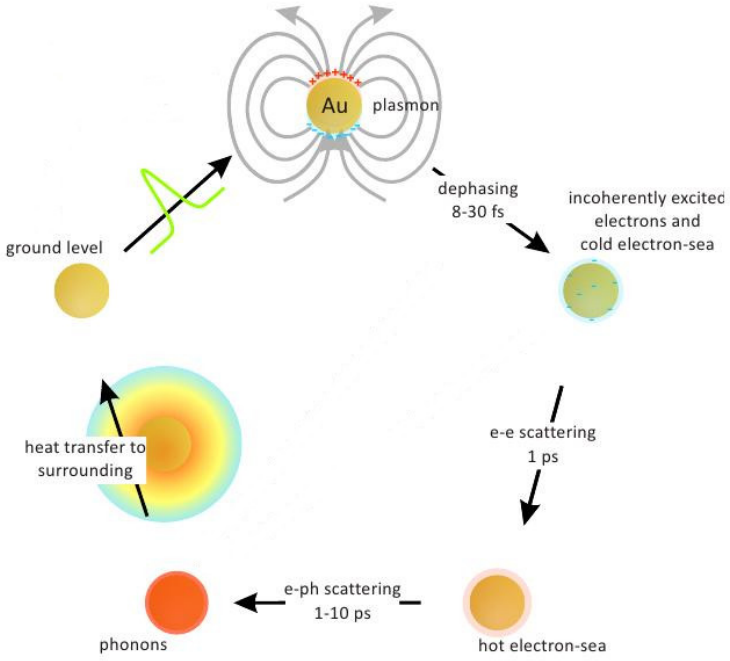

Figure 4: Relaxation of nanoparticles after femtosecond pulse excitation [1].

Example OKE signal for the nanorods covered with CTAB, suspended in water is given in Fig 3, whereas the evolution of the excited nanoparticles is presented in Fig 4. The initial spike in the signal is due to the hyperpolarizability of water. The decomposition of the signal into water and nanorods components is given in Fig 7 for short delay range. The observed initial nanorods signal build up is due to the intraband absorption at the edge of the longitudinal plasmon resonance. As this absorption is dependent on the relative orientation of the nanoparticle with respect to the pump pulse polarization, the nanoparticles oriented along the pump polarization direction are most effectively excited (see Fig 6, c). The decoherence of the excited electrons is very fast, comparable with the pulse duration, therefore in OKE it happens during the initial build up of the nanoparticles signal. The shape of the initial build up depends only on the shape of the laser pulse (see Fig 9, left). The obtained electron energy distribution does not correspond to an equilibrium and the energy is redistributed among the electrons during the electron-electron relaxation. As some energy was absorbed from the laser pulse, the obtained Fermi-Dirac distribution corresponds to a higher temperature than before the excitation. The transition of the electron energies distribution to the Fermi-Dirac distribution is observed in the signal for higher pump pulse energies as an additional, slower component of signal

build up (see Fig 9, right). The excitation of the electrons results in perturbation of the longitudinal and transverse polarizability of the nanorods, which combined with orientational selectivity, results in sample anisotropy, detected in OKE.

In Fig 3, the signal decay shows a fast and a slow component. The fast decay of the signal is due to electron-phonon relaxation, where the energy from the hot electrons is transferred to the crystal lattice. The electron-phonon relaxation shows a decay rate, which is pump pulse energy dependent (see Fig 9, right), due to the electron heat capacity temperature dependence $C_e = \gamma T_e$:

$$\frac{\partial T_e}{\partial t} = -\frac{g}{\gamma T_e}\left(T_e - T_l\right) \tag{1}$$

$$\frac{\partial T_l}{\partial t} = \frac{g}{C_l}\left(T_e - T_l\right) - \frac{1}{\tau_s}\left(T_l - T_0\right) \tag{2}$$

$$\tag{3}$$

where g is the electron-phonon coupling constant, C_l is the lattice heat capacity, τ_s is the lattice cooling time constant, T_e, T_l and T_0 are the electrons, lattice and environment temperatures, respectively.

Lattice heating results in change of the rod equilibrium dimensions. Modified rod dimension results in modified polarizability, hence the relaxation of the equilibrium dimension, corresponding to the energy transfer to the solvent, is observed as a slow exponential decay (phonon-phonon relaxation). Cooling time of nanoparticle strongly depends on environment thermal conductivity, surfactant particles and nanoparticle radius $\sim R^2$. In water and silica the relaxation time is about 100 ps for 20 nm gold nanospheres [2].

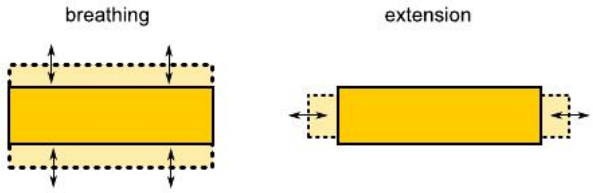

Figure 5: Diagram showing the fundamental extensional and breathing modes of a long cylindrical rod. The breathing mode exhibits a pure radial expansion and contraction without a change in length. In the extensional mode, an increase in length is accompanied by a decrease in width [2].

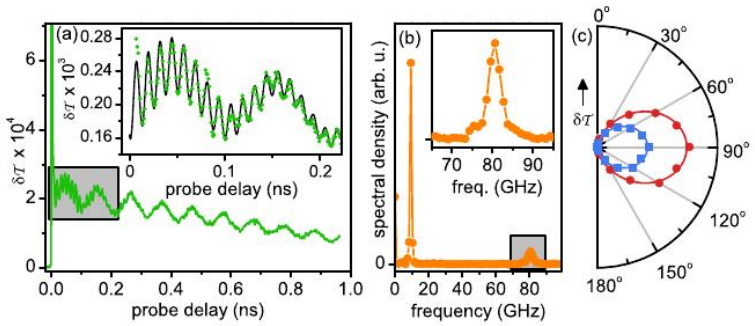

Figure 6: Single 29x90 nm nanorod vibrational trace (a) Vibrational trace of a single gold rod. Inset: zoom on the highlighted part, fitted with Eq. 3.3. (b) Power spectral density of the trace in (a) after Fourier transform (inset: zoom on the high-frequency peak). (c) Polarization dependence of the optical response amplitude for the breathing (squares) and the extensional mode (circles), with cosine fits (solid lines) [2].

If the acoustic vibrations of the nanorods show period longer than the electron-phonon relaxation time, then the sudden energy transfer from electrons to the lattice results in all of the nanorods being in out of equilibrium position, which results in coherent (phase-synchronized) vibrations, which also modulate the anisotropy. This is analogous to a situation, where we suddenly shift the fix point of a pendulum. There are two acoustic modes, that can be coherently excited - extensional and breathing (Fig 5, Fig 6), where the latter is not visible in OKE. The decay of oscillations in the signal depends on

the nanoparticles size dispersion (different nanoparticle sizes result in different vibration frequencies). The vibration frequency of the polycrystalline nanorods depends only on the aspect ratio:

$$\frac{\nu_{br}}{\nu_{ext}} = 2.32AR. \tag{4}$$

For nanocrystals the growth direction has to be considered.

2.1 Signal build up analysis

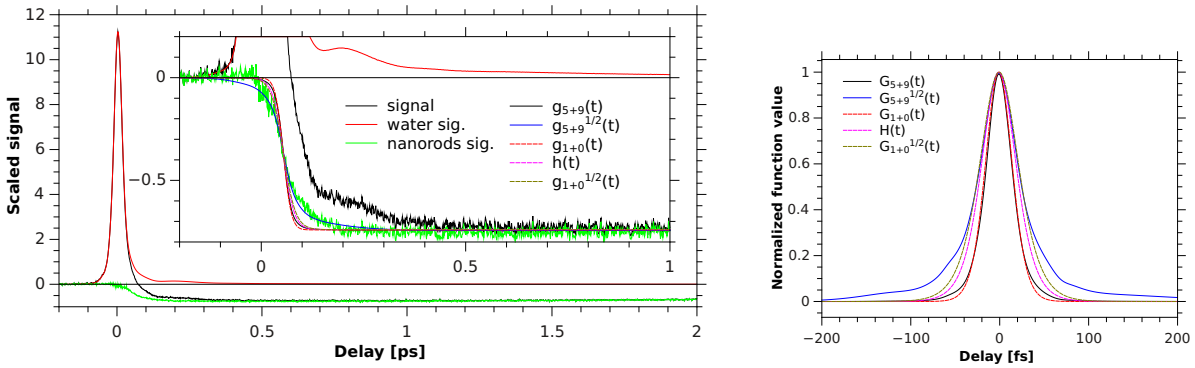

Figure 7: (Left) – Decomposition of experimental signal into water and nanorods contributions, the inset shows also models for the nanorods signal initial build up; (Right) – Convolutions used for obtaining the signal build up.

The initial build up of the nanoparticles signal is not well modelled by the integral of the cross-correlation of pump and probe pulse intensities (see Fig 7), which would correspond to the convolution of this correlation with a step function:

$$g(\tau) = \int_{-\infty}^{\infty} G(\tau - t)\Theta(t)dt = \int_{0}^{\infty} G(\tau - t)dt = \int_{-\infty}^{\tau} G(t')dt' \tag{5}$$

$$G(\tau) = \int_{-\infty}^{\infty} I_p(t + \tau)I_{pr}(t)dt \tag{6}$$

$$\Theta(t) = \begin{cases} 0 & t < 0 \\ 1 & t \geq 0 \end{cases} \tag{7}$$

This model is appropriate for the off-resonant measurements, where the birefringence is proportional to the square of electric field. This results from:

- electron cloud hyperpolarizability

$$\hat{\alpha} = \hat{\alpha}_0 + \hat{\gamma} \cdot \vec{E} : \vec{E} \tag{8}$$

- minute orientation of anisotropic molecules by the field, where the torque on the molecule is due to the interaction of the field and dipole moment induced by this field:

$$\vec{\tau} = \left(\hat{\alpha}_0 \vec{E}\right) \times \vec{E} \tag{9}$$

- coherent molecular vibrations, where the oscillation driving force and thus its amplitude is proportional to field squared (derivation can be found in [3]). In general it is obtained by solving the harmonic oscillator equation, where the driving force is obtained from the derivative of potential energy of a dipole moment induced by field at frequency ω_a in the presence of field at frequency ω_b. The resulting differential equation is:

$$\ddot{q} + \gamma\dot{q} + \omega_0^2 q = \frac{F}{\mu} = \frac{1}{\mu}\left[\left(\frac{\partial\hat{\alpha}}{\partial q}\right)_{q=0} \vec{E}_0(\omega_a)\right] \vec{E}_0(\omega_b)\frac{1}{4}\left[e^{i(\omega_a - \omega_b)t} + c.c.\right], \tag{10}$$

The oscillation normal coordinate is then written for resonance ($\omega_a - \omega_b = \omega_0$) as:

$$q = \frac{1}{\mu}\left[\left(\frac{\partial\hat{\alpha}}{\partial q}\right)_{q=0} \vec{E}_0(\omega_a)\right] \vec{E}_0(\omega_b)\frac{1}{4}\frac{1}{\gamma(\omega_a - \omega_b)}\left[e^{i\left[(\omega_a - \omega_b)t - \frac{\pi}{2}\right]} + c.c.\right], \tag{11}$$

In the case of nanoparticles the field frequency is on the edge of plasmon resonance. The electron cloud oscillation can be obtained from the Drude-Sommerfeld theory by solving the following equation of motion for the electrons:

$$\ddot{q} + \gamma\dot{q} = \frac{F}{m_e} = -\frac{1}{m_e} e\vec{E}_0 \frac{1}{2}\left[e^{i\omega t} + c.c.\right], \tag{12}$$

The solution is:

$$q = \frac{1}{m_e}\vec{E}_0 \frac{1}{2}\left[\frac{1}{\omega^2 - i\omega\gamma} e^{i\omega t} + c.c.\right]. \tag{13}$$

From the above equations one can see that the birefringence will depend on the pulse field envelope, therefore the signal build up should be calculated using the integral of the following cross-correlation function:

$$H(\tau) = \int_{-\infty}^{\infty} I_p^{\frac{1}{2}}(t+\tau) I_{pr}(t) dt \tag{14}$$

Unfortunately in the OKE experiment only the $G(t)$ function can be measured. A good fit of this function was obtained with 5 autocorrelations of sech^2 function and 9 Gaussians (index 5+9 in Fig 7. A fit was also made with a single sech^2 autocorrelation:

$$G_{1+0}(t) = 3H \frac{1.76\frac{t}{t_{\mathrm{FWHM}}}\cosh(1.76\frac{t}{t_{\mathrm{FWHM}}}) - \sinh(1.76\frac{t}{t_{\mathrm{FWHM}}})}{(\sinh(1.76\frac{t}{t_{\mathrm{FWHM}}}))^3} \tag{15}$$

This fit was used in order to obtain the corresponding sech^2 shape and to calculate the $H(t)$ cross-correlation function. As shown in Fig 7, the square root of $G(t)$ can be used as a relatively good approximation of $H(t)$. Indeed the integral of square root of the precise fit of the cross-correlation gives a good approximation of the signal build up. There is only one unsolved issue - the integrals need to be shifted by 55 fs in order to overlap with the signal. The reason for this time lag is not understood.

The above conclusions are confirmed by the experiment performed at different pump power levels. In Fig. 8 the OKE measurements normalised to the pump power show a decreasing nanoparticles response compared to that of water, whereas the signals after scaling by square root of power show a comparable nanorods signal amplitude.

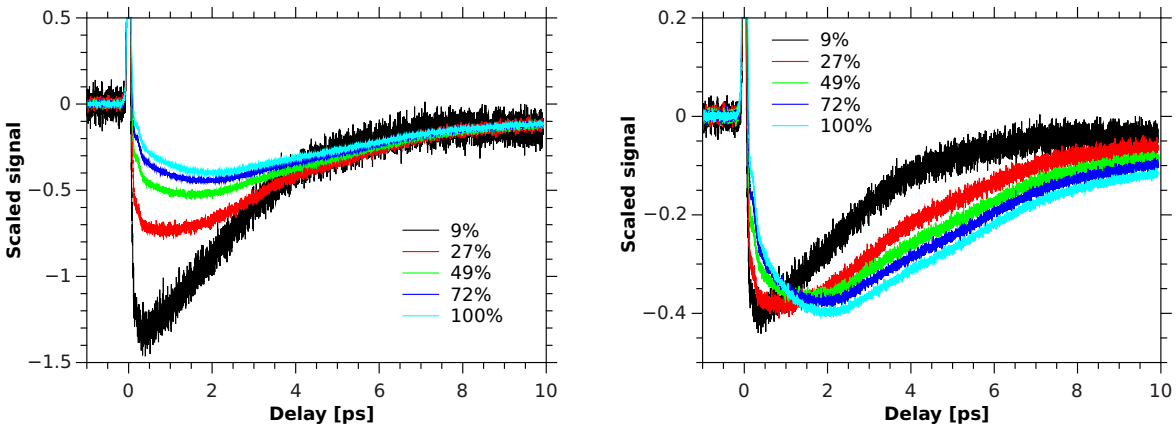

Figure 8: (Left) – Signals normalized to the pump power (Right) – Signals normalized to the square root of the pump power.

In Fig 9 the power dependent signals are given after water component subtraction and normalization to the initial signal build up. As can be seen the initial signal build up is rather power independent within the precision of water component removal. The electron-phonon relaxation slows down with increasing pump power, which is due to strong temperature dependence of the thermal capacity of the electrons. Also with increasing power an additional, slower signal build up component is observed, after the pump pulse. This is due to the thermalization of the hot electrons.

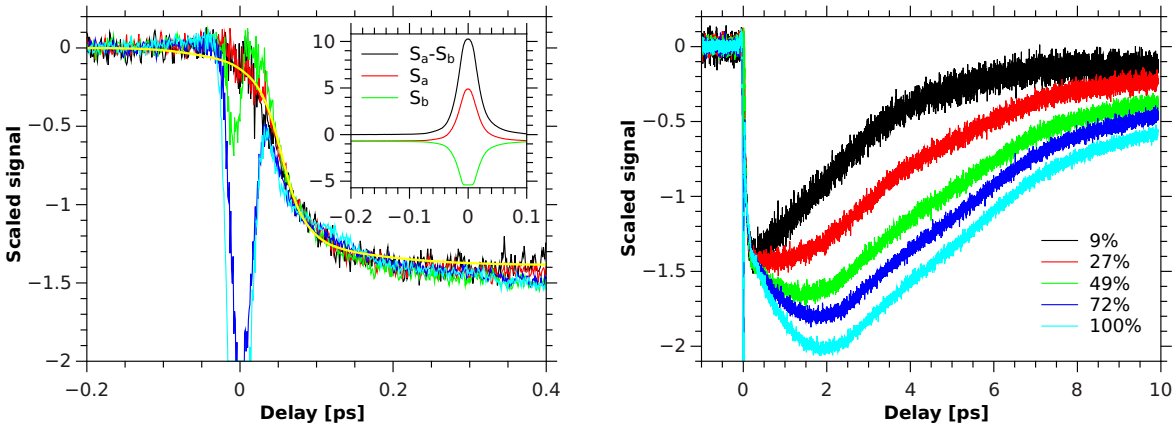

Figure 9: Signal after water component subtraction, normalized to the initial build up; (Left) – initial build up, the spikes around zero are artefacts obtained while subtracting water signal, due to detector saturation during measurement at high power (see inset), the yellow line is the model build up obtained from integration of square root of pump-probe intensity cross-correlation function; (Right) – the electron-electron and electron-phonon relaxation range.

2.2 Nanoparticles melting

If too much energy is pumped into the nanoparticles, they melt. The melting process starts at the surface and surface melting temperature decreases with size. For < 5 nm nanoparticles melting temperature scales as R^{-1}. The core melts at bulk material melting temperature. Reversible surface melting and irreversible core melting were investigated with optical-pump X-ray probe technique and revealed the 100 ps melting process [2]. Laser induced heating influences also elastic constants and thus acoustic frequencies of the nanoparticle. Surface melting (due to sample resistive heating) result in sudden change of decoherence time and phase of the oscillations [2]. Nanorods show surface melting at 40 % of the melting point when continuously heated. Energy from laser pulses is lost to the environment, therefore femtosecond pulses are more effective than nanosecond ones [2].

2.3 Nanoparticles applications

- selective heating of tumor/bacteria/parasite cells (absorption region can be tuned as needed)
- core-shell nanoparticle drug delivery with shell melting release
- heating of thermo-responsive materials
- laser induced phase transitions in NP doped materials (like CD-RW alloy)
- optical recording by laser induced micro-explosions
- dichroic material created by polarisation selective reshaping of nanorods with laser light

3 Literature references

[1] A. S. Urban, *Ph.D. thesis*, Physics Department of the Ludwig-Maximilians-Universität München, 2010.

[2] P. Zijlstra, *Ph.D. thesis*, Centre for Micro-Photonics Faculty of Engineering and Industrial Sciences Swinburne University of Technology Melbourne, Australia, 2009.

[3] K. Polok, in *Fizykochemiczne metody badawcze w nano- i biotechnologii*, ed. M. Szklarczyk, Wydawnictwa Uniwersytetu Warszawskiego, 2015, ch. 11.